Journal of Molecular Liquids 269 (2018) 152–159

Contents lists available at ScienceDirect

Journal of Molecular Liquids

journal homepage: www.elsevier.com/locate/molliq

CFD modeling of turbulent convection heat transfer of nanofluids containing green functionalized graphene nanoplatelets flowing in a horizontal tube: Comparison with experimental data

Rad Sadri [a,*], A.R. Mallah [a], Maryam Hosseini [a], Goodarz Ahmadi [b], S.N. Kazi [a], Ali Dabbagh [c,d], C.H. Yeong [c], Roslina Ahmad [a], N.A. Yaakup [e]

[a] Department of Mechanical Engineering, Faculty of Engineering, University of Malaya, Kuala Lumpur 50603, Malaysia
[b] Department of Mechanical and Aeronautical Engineering, Clarkson University, Potsdam, NY 13699, USA
[c] School of Medicine, Faculty of Health and Medical Sciences, Taylor's University, Subang Jaya 47500, Malaysia
[d] Department of Materials Science and Engineering, Sharif University of Technology, Tehran, Iran
[e] Department of Biomedical Imaging, Faculty of Medicine, University of Malaya, Kuala Lumpur, 50603, Malaysia

ARTICLE INFO

Article history:
Received 3 April 2018
Received in revised form 30 May 2018
Accepted 4 June 2018
Available online 5 June 2018

Keywords:
Nanofluids
Eco-friendly functionalization
Convective heat transfer
Turbulent flow
CFD modeling
Friction factor
Graphene nanoplatelets
SST k-ω

ABSTRACT

In this research, a series of numerical simulations were conducted utilizing computational fluid dynamics (CFD) software in order to predict the heat transfer performance of queues nanofluids containing clove-treated graphene nanoplatelets (CGNPs) flowing in a horizontal stainless steel heated pipe. The GNPs were covalently functionalized with clove buds using free radical grafting reaction using an eco-friendly process. The advantage of this synthesis method was that it did not use hazardous acids, which are typically used in traditional treatment methods of carbon nanostructures. The thermo-physical properties of the aqueous nanofluids obtained experimentally were used as inputs for the CFD simulations for solving the governing equations of heat transfer and fluid motion. The shear stress transport (SST) k-ω turbulence model was also used in these simulations. The corresponding convective heat transfer coefficient and friction factor of aqueous nanofluids for nanoparticle weight concentrations of 0.025, 0.075, and 0.1% were evaluated. The simulation results for both heat transfer coefficient and friction factor were shown to be in agreement with the experimental data with an average relative deviation of about ±10%. The presented results confirmed the applicability of the numerical model for simulating the heat transfer performance of CGNPs aqueous nanofluids in turbulent flow regimes.

1. Introduction

There has been considerable interest in developing working fluids with good thermal properties for increasing heat transfer efficiency of heat exchangers [1–5]. Recent studies on nanofluids showed that adding small amount of highly thermally conductive nanoparticles in the base fluid (e.g. water) enhances the thermal conductivity, hence enhancing the convective heat transfer rate of base fluid [6–17]. Actually, the reduction of the thermal boundary layer thickness caused by the presence of the nanoparticles and their random motion within the base fluid may have significant effect to such convective heat transfer coefficient improvement as well [18–20]. Typically, the heat transfer rate of the base fluid increases by increasing the nanoparticle concentration. This is because the increase of nanoparticle concentration increases the Brownian motion induced fluctuations in the fluid that results in the rapid heat transfer from the wall to nanofluid. In order to reduce costs associated with experimental studies, much effort has been made to use numerical simulations to examine the performance of nanofluids on convective heat transfer in various applications. In this regard, both two-phase and single-phase simulation models have been developed for studying convective heat transfer of thermal systems where nanofluids are used as the working fluids. Single phase (homogeneous) models are popular for numerical studies involving aqueous nanofluids due to the simplicity of these models. In this approach, the nanoparticles are supposed to be homogeneously distributed in the base fluid [21]. The effective thermophysical characteristics, containing specific heat capacity, thermal conductivity, dynamic viscosity and density, are then evaluated based on the mixture model of nanoparticles and base fluid. In addition, the effective single-phase model assumes that the liquid and solid particle phases are in chemical and thermal equilibrium, and there is no relative velocity between the phases [22–24]. By its nature, the single-phase modeling is generally easier and less time-consuming compared with two-phase modeling. However, it is crucial to apply suitable equations in order to compute the properties of single-phase nanofluids [25].

* Corresponding author.
E-mail address: rod.sadri@gmail.com (R. Sadri).

https://doi.org/10.1016/j.molliq.2018.06.011
0167-7322/

In two-phase modeling, it is assumed that there are slip velocities between the nanoparticles and base fluids. For this reason, the nanofluids are treated as inhomogeneous mixtures and there are variations in the nanoparticle concentration in nanofluids. Due to its simplicity, a large number of numerical studies have been accomplished for predicting the convective heat transfer and hydrodynamic characteristics of aqueous nanofluids using single-phase models with an acceptable degree of accuracy [26]. Jayakumar et al. [27] conducted CFD modeling and experimental studies in a fluid to fluid heat exchanger in order to compare the thermal and flow properties inside a helical coil for different boundary conditions. They investigated the impact of using constant fluid characteristics using standard k–ε turbulence model in the computational modeling of heat transfer by comparing the data with those obtained for constant properties. They found that the predicted results match reasonably good with the experimental data. Conte et al. [28,29] performed both numerical and experimental studies to understand convective heat transfer from a single round pipe coiled in a rectangular pattern. The focus was addressed on exploring the flow pattern and temperature distribution through the pipe. The results of both experimental and numerical investigations show better heat transfer performance.

Maiga et al. [30] have studied the problem of forced convection, turbulent and laminar, inside a uniformly heated tube, indicating the heat transfer enhancement is caused by the inclusion of nanoparticles. Lotfi et al. [31] compared the two-phase Eulerian model and Mixture model with the single phase model for convection Al_2O_3 aqueous nanofluid in horizontal tubes and the data represented that the mixture model had better Nusselt number(Nu) predictions. The single-phase model also was employed by Nambura et al. [24], and Maiga et al. [30] and Akbarnia and Behzadmehr [32] for the study of convection heat transfer of different aqueous nanofluids inside the circular pipes. Based on their results, the single-phase model gives the sensible results for the aqueous nanofluids. Kumar et al. [33] have modelled the heat transfer and fluid flow in a tube-in-tube helically coiled heat exchanger for various fluid flow rates in the outer and inner tube. The renormalization group (RNG) k–ε is employed to simulate the heat transfer and turbulent flow in the heat exchanger. It was discovered that the overall convective heat transfer coefficient elevates by increasing the inner-coiled tube flow rate for a constant flow rate in the annulus region. Similar trends in the variation of overall convective heat transfer coefficient were discovered for various flow rates in the annulus region for a constant flow rate in the inner-coiled tube. Besides, it was figured out that the overall heat transfer coefficient also increases by increasing the operating pressure in the inner tube. The friction factor values in the inner-coiled tube were in consent with the literature results. Di Piazza et al. [34] numerically investigated heat transfer and turbulent flow in curved tubes, representative of helically coiled heat exchangers. Alternative CFD turbulence models (RSM–ω, SST k–ω and k–ε) were compared with direct numerical simulation results and heat transfer data and experimental pressure drop. The data showed that utilizing the RSM–ω and SST k–ω turbulence models, pressure loss data were in good consent with the literature results and the Ito correlation. For convective heat transfer, the literature was not comparably accurate or complete, however, a well agreement was achieved in the range of available results.

Goodarzi et al. [35] conducted a numerical study using a FORTRAN code to investigate the pressure loss and convective heat transfer of a counter flow corrugated plate heat exchanger in which the nanofluids containing MWCNTs that functionalized via mixture of HNO_3/H_2SO_4 used as coolants. They indicated that loading of nanoparticles can increase the convective heat transfer coefficient of the base fluid. Besides, it was figured out that increasing the nanoparticle volume fraction as well as reduction of Peclet number could add to the friction factor which in turn leads to increase the pumping power and pressure drop. They showed that the density and thermal conductivity play important role in the betterment of heat exchanger efficiency.

Most of the previous studies involved nanoparticles functionalized using corrosive and hazardous acids. To the best of our knowledge, there are no notable numerical researches regarding heat transfer and hydrodynamic characteristics of nanofluids containing GNPs covalently functionalized using an eco-friendly functionalization method are chosen as the working fluids. In this study, a computational modeling of flow and heat transfer of nanofluids including green functionalized GNPs in a horizontal circular tube was carried out using the ANSYS-Fluent computational fluid dynamics (CFD) software. A three-dimensional model was constructed and the turbulent flow conditions were evaluated using the SST *k-ω* model. The nanofluids were composed of several CGNP concentrations (0.025, 0.075 and 0.1 wt%) in the distilled (DI) water. Simulations were conducted for Reynolds numbers ranging from 6371 to 15,927. A constant heat flux of 12,752 W/m^2 at the channel walls was imposed as the boundary condition. A single-phase model under steady-state condition was used, and the simulation results were compared with the earlier experimental data [36] for model validation and text of accuracy.

2. Numerical simulations

A computational fluid dynamics methodology was employed to study the thermal performance of a horizontal circular heated tube containing clove-treated GNPs nanofluids under steady fully developed turbulent flow condition. Fig. 1 shows the schematic of the heated horizontal circular pipe configuration. The total length of the tube is 1.4 m, the heated section length is 1.2 m, and the inner diameter of the pipe is 10 mm. The tube was subjected to a constant heat flux of 600 W. The commercial CFD software, ANSYS-Fluent v18, installed in a computer with Intel® Core™ i7-4770 3.40 GHz processor and 16 GB of random access memory, was used for these simulations. The grid was generated using meshing module provided by the software package. In this model, only the fluid control volume was modelled and the thickness of tube wall was not considered. The structured grids with 9 inflation layers was employed to mesh the region close the walls where large gradients of velocity and temperature occur. Unstructured grid was used for the interior volume cells. The computational grid is shown in Fig. 2. Experimental apparatus details are described in the Fig. S1 (a) and (b) of the Supplementary material.

It was assumed that the working fluids are homogeneous single-phase nanofluids, which implies that the CGNPs nanoparticles and base fluid (DI water) have the same local temperature. The properties of the nanofluid were obtained empirically [36], the effective single-phase flow model was used in the analysis. It was also assumed that the nanofluid is a Newtonian fluid with material properties that are functions of concentration. The temperature dependence of thermophysical was neglected as the temperature variations were relatively small in the present study.

The steady-state governing equations of conservation of mass, balance of momentum, and conservation of energy for single-phase effective model as presented in [37,38] are:

Conservation of mass:

$$\nabla \cdot \left(\rho \vec{V}\right) = 0 \tag{1}$$

Conservation of momentum:

$$\nabla \cdot \left(\rho \vec{V}\ \vec{V}\right) = -\nabla P + \nabla \cdot \left[(\mu + \mu_t)(\nabla \vec{V} + \nabla \vec{V}^T)\right] + \rho \vec{g} \tag{2}$$

Conservation of energy:

$$\nabla \cdot \left(\rho C_p\ \vec{V} T\right) = \nabla \cdot (K_{eff} \nabla T) + \rho \epsilon \tag{3}$$

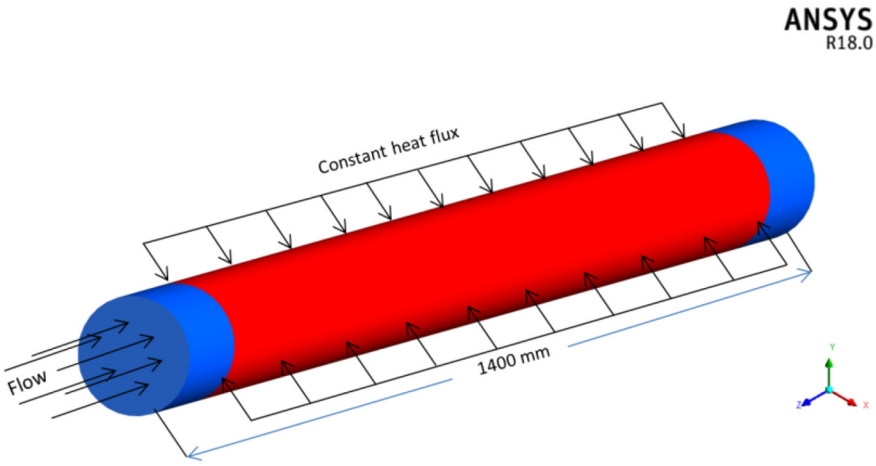

Fig. 1. The 3D model of horizontal circular heated tube.

where $\vec{V}$ is the mean velocity vector, $K_{eff} = K + K_t$ is the effective thermal conductivity of a homogeneous single-phase fluid, and ϵ is the energy dissipation rate.

For a range of CGNP concentrations, the effective thermo-physical properties of the nanofluid including density, ρ, viscosity, μ, specific heat capacity, C_p, and thermal conductivity, K as measured in experimental study [36] for a temperature of 30 °C, as listed in Table 1 were used in these simulations.

The boundary conditions for solving the governing equations for CFD model are described in this section. Uniform heat flux and no-slip boundary condition were employed for the tube walls. The fluid enters the tube at a constant inlet temperature $T_{in} = 303.15$ K and uniform axial velocity V_{in}. The velocity and temperature were assumed to be fully developed at the inlet of the tube. It was assumed that the tube walls were perfectly smooth and the external surface of the tube walls was insulated. As noted before, for the no-slip boundary condition $V_{wall} = 0$ on the tube wall. The acceleration of gravity was set as 9.8 m/s^2. Three CGNP concentrations of 0.025, 0.075, and 0.1 wt% were considered in these simulations. At the outlet of the pipe, the out flow condition was imposed.

In this study, the turbulent nanofluid flow inside the horizontal tube was simulated for the Reynolds number range of 6371–15,927. The

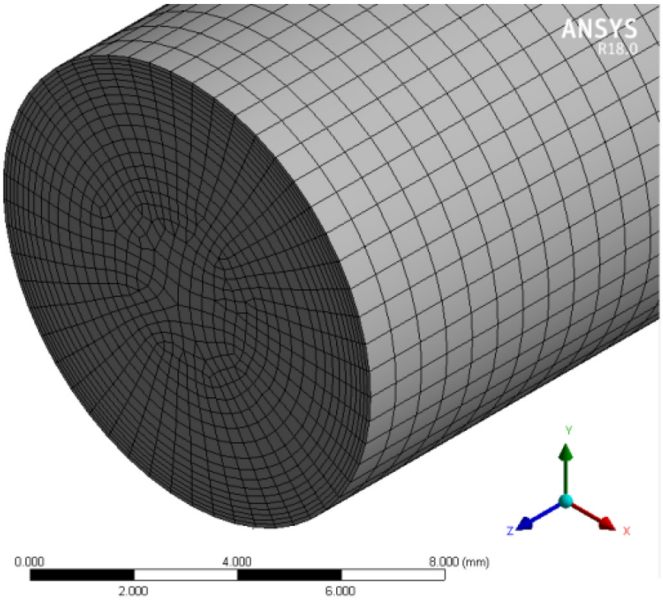

Fig. 2. Grid of the solution domain.

two-equation shear stress transport (SST k-ω) turbulence model proposed by Menter [39] was used in these simulations and for determining the convective heat transfer coefficient. The governing equations for the SST k-ω turbulent model are given as,

$$U_j \frac{\partial \rho k}{\partial x_j} = \tau_{ij} \frac{\partial u_i}{\partial x_j} - \beta^* k \rho \omega + \frac{\partial}{\partial x_j}\left[(\mu + \sigma_k \mu_t)\frac{\partial k}{\partial x_j}\right] \tag{4}$$

$$U_j \frac{\partial \rho \omega}{\partial x_j} = \frac{\gamma}{v_t}\tau_{ij}\frac{\partial u_i}{\partial x_j} - \beta \omega^2 + \frac{\partial}{\partial x_j}\left[(\mu + \sigma_\omega \mu_t)\frac{\partial \omega}{\partial x_j}\right] + 2(1-F_1)\rho\sigma_{\omega 2}\frac{1}{\omega}\frac{\partial k}{\partial x_j}\frac{\partial \omega}{\partial x_j} \tag{5}$$

The default values for the SST k-ω model parameters were used for these simulations [39]. These are,

$$\sigma_{k1} = 0.5, \sigma_{\omega 1} = 0.5, \beta_1 = 0.075, \beta^* = 0.09, \kappa = 0.41, \gamma_2 = \beta_2/\beta^* - \sigma_{\omega 2}\cdot K^2/\sqrt{\beta^*}$$

where,

$$v_t = \frac{k}{\omega} \tag{6}$$

The turbulent stress tensor is given as,

$$\tau_{ij}^t = \mu_t\left(\frac{\partial u_i}{\partial x_j} + \frac{\partial u_j}{\partial x_i} - \frac{2}{3}\frac{\partial u_k}{\partial x_k}\delta_{ij}\right) - \frac{2}{3}\rho k \delta_{ij} \tag{7}$$

In Eq. (5),

$$F_1 = \tanh(arg_1^4) \tag{8}$$

where,

$$arg_1 = \min\left[\max\left(\frac{\sqrt{k}}{0.09\omega y}; \frac{500\nu}{y^2\omega}\right); \frac{4\rho\sigma_{\omega 2}k}{CD_{k\omega}y^2}\right] \tag{9}$$

where y is the distance to the solid surface and $CD_{k\omega}$ is the positive portion of the cross-diffusion term that can be determined from the following equation:

$$CD_{k\omega} = \max\left(2\rho\sigma_{\omega 2}\frac{1}{\omega}\frac{\partial k}{\partial x_j}\frac{\partial \omega}{\partial x_j}, 10^{-20}\right) \tag{10}$$

Table 1
Thermo-physical characteristics of the water and CGNP aqueous nanofluids at an inlet temperature of 30 °C [36].

Thermo-physical properties	DI water 0 wt%	CGNPs 0.025 wt%	CGNPs 0.075 wt%	CGNPs 0.1 wt%
Thermal conductivity (W/m·K)	0.611	0.636	0.681	0.708
Viscosity (mPa·s)	0.829	0.844	0.868	0.885
Specific heat capacity (J/kg·K)	4142	4123	4096	4080
Density (kg/m^3)	995.50	995.6	995.8	995.9

The set of differential equations (governing equations) was discretized using the finite-volume approach and solved iteratively by utilizing the line-by-line procedure. The second order upwind scheme was employed for the convective and diffusive terms whereas the algorithm of SIMPLEC was used for the velocity-pressure coupling [40]. For the convergence criteria, the sum of the scaled absolute residuals for the parameters of mass and velocity were restricted to $<10^{-3}$ and temperature was restricted to $<10^{-6}$.

In order to ensure that the simulations were independent of the grid size, grid independency tests were carried out for three grid sizes. We have plotted the number of nodes against *Nu* number (Fig. 3(a)) and ΔP (Fig. 3(b)). It can be seen from Fig. 3(a) and (b) that a grid with about 2,000,000 elements provides satisfactory results for the *Nu* and pressure drop. Increasing the grid size beyond 2,000,000 elements does not significantly influence the accuracy of the results. Based on these observations, the optimal grid of 2,000,000 cells was selected for the subsequent computations.

More details on the effect of grid size on the *Nu* number and pressure drop are presented in the Tables S1 and S2 of the Supplementary material, respectively.

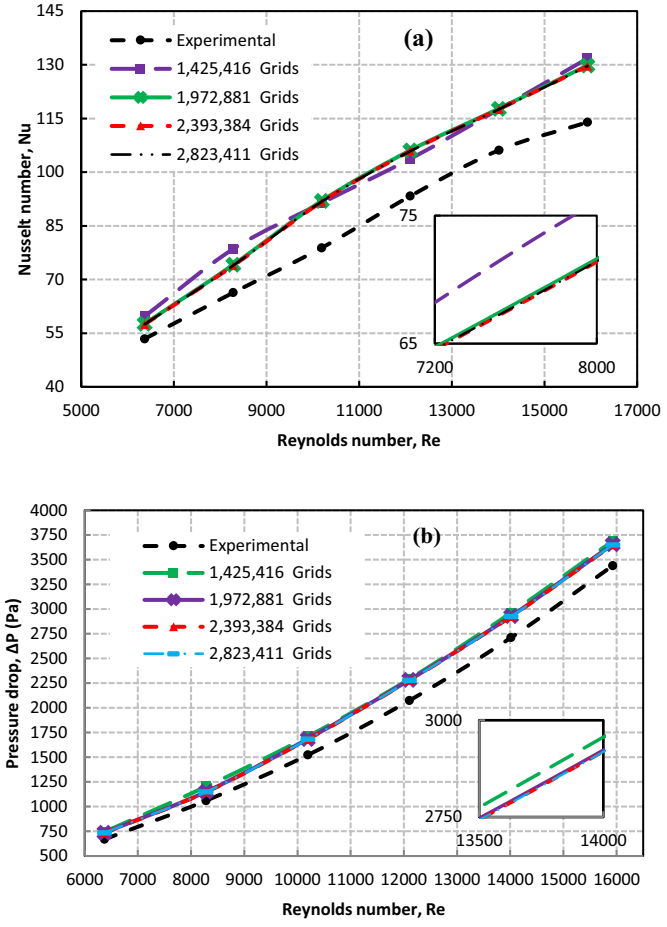

Fig. 3. Grid independency tests. (a) Variations of *Nu* number and (b) pressure drop as a function of the *Re* number. Comparison with the experimental data of [36].

Once the convergence was achieved, the wall and bulk temperatures and the shear stress results along the heated tube were evaluated. The corresponding friction factor (f), pressure drop (ΔP), local and average convective heat transfer coefficients (h), and Nusselt number (Nu) were then computed using the following equations:

$$f = \frac{8\tau_w}{\rho v^2} \tag{11}$$

$$\Delta p = \frac{4L\tau_w}{D} \tag{12}$$

$$\overline{h} = \frac{q}{T_w - T_b} \tag{13}$$

$$h_{(x)} = \frac{q}{T_{w_{(x)}} - T_{b_{(x)}}} \tag{14}$$

$$\overline{Nu} = \frac{\overline{h} \cdot D}{k} \tag{15}$$

$$Nu_{(x)} = \frac{h_x \cdot D}{k} \tag{16}$$

where, τ_w, v, ρ, h, q, D, k, T_b, and T_w represent the wall shear stress, flow velocity, fluid density, convective heat transfer coefficient, heat flux, inner tube diameter, thermal conductivity of the fluid, bulk temperature over the heated zone, and wall temperature, respectively.

3. Results and discussion

In order to ensure the accuracy of the CFD model and the numerical procedure, the simulations were carried out using the same geometry and dimensions of the experimental horizontal circular heated tube and under the same operating conditions as those used in the experimental study of [36]. The predicted average *Nu* for DI water inside the horizontal tube subjected to uniform heat flux were compared to those determined from the experiments [36] and empirical correlations proposed by Petukhov [41] (Eq. (17)), Gnielinski [42] (Eq. (18)), and Notter-Rouse [43,44] (Eq. (19)), and the results are plotted in Fig. 4(a).

$$Nu = \frac{\left(\frac{f}{8}\right) RePr}{1.07 + 12.7\left(\frac{f}{8}\right)^{0.5}\left(Pr^{2/3} - 1\right)} \tag{17}$$

Eq. (17) was used if $3000 < Re < 5 \times 10^6$ and $0.5 \le Pr \le 2000$.

$$Nu = \frac{\left(\frac{f}{8}\right)(Re - 1000)\, Pr}{1 + 12.7\left(\frac{f}{8}\right)^{0.5}\left(Pr^{\frac{2}{3}} - 1\right)} \tag{18}$$

here, Pr is the Prandtl number and f is the friction factor. Eq. (18) was used if $3 \times 10^3 < Re < 5 \times 10^6$ and $0.5 \le Pr \le 2000$.

$$Nu = 5 + 0.015\, Re^{0.856}\, Pr^{0.347} \tag{19}$$

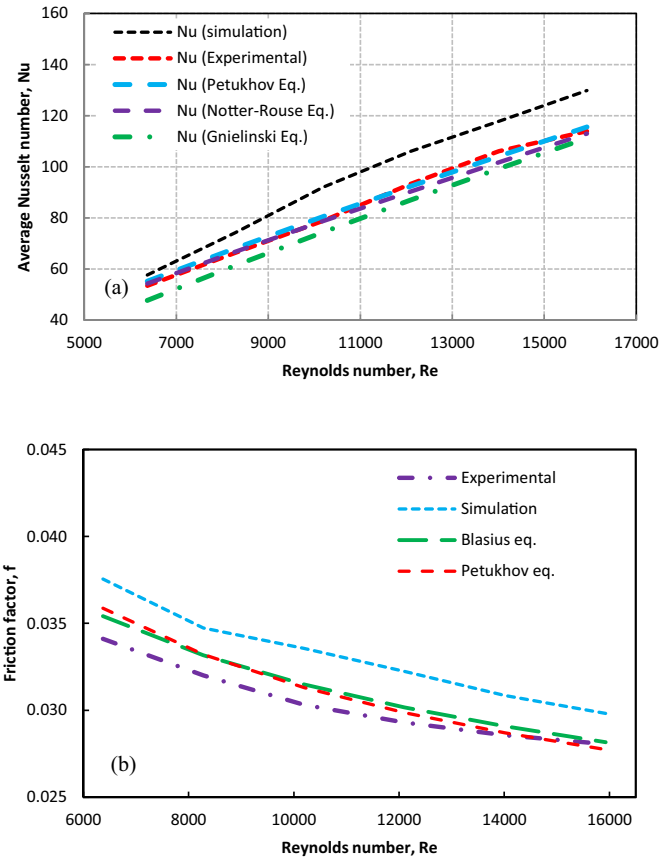

Fig. 4. Comparison of the (a) Nusselt number and (b) friction factor between simulation, experiment, and empirical correlations for DI water.

The friction factor (f) in Eqs. (17) and (18) were determined using the relationship proposed by Petukhov [41]:

$$f = (0.79\,Ln\;\;Re - 1.64)^{-2} \tag{20}$$

Fig. 4 shows that there is good agreement between the simulation data and the experimental data those obtained from Notter-Rouse's and Petukhov's empirical correlations, with an average relative deviation of 12.48, 13.72, and 11.31%, respectively. This may be due to the existence of conduction resistance in the experimental test section, which was not considered in the CFD model. Also, there are deviations might be resulted from implementation of the approximating models of turbulence on one hand, and the error of the measuring instruments in the experimental on the other hand. Based on the results, it can be deduced that the CFD model is capable of simulating the heat transfer characteristics of the CGNP-DI water nanofluids.

The predicted friction factors for DI water were compared with those determined from experimental data and empirical correlations proposed by Petukhov [41] and Blasius [45] (which are given by Eqs. (20) and (21), respectively) and the results are plotted in Fig. 4(b).

$$f = 0.3164\;\;Re^{-0.25} \tag{21}$$

This equation is valid for $3000 < Re < 10^5$.

The results are indeed encouraging since the average relative deviations in the friction factor between the simulations and those obtained from experiments and Petukhov's [41] and Blasius's [45] empirical correlations are 8.94, 6.024, and 6.56%, respectively. This indicates that the CFD model is reliable to measure the hydrodynamic properties of CGNP-DI water nanofluids within the range of Reynolds number investigated in this study.

Fig. 5 shows the axial local *Nu* number for DI water as a function the Reynolds number. It can be observed that the local Nusselt number decreases by increasing the axial distance along the horizontal tube, though the local *Nu* seems to be invariant when *X*/*D* is more than 15. It is apparent that there is a significant drop in the local *Nu* number when *X*/*D* is within a range of 0–15. The local *Nu* number remains relatively constant thereafter due to the fully developed turbulent flow condition. In addition, it is evident that increasing the Reynolds number reduces the temperature difference between the bulk and wall temperature which results in higher convective heat transfer coefficient and thus, higher *Nu*.

A series of CFD simulations using the effective single-phase model were performed in order to predict the convective heat transfer coefficient and pressure drop of the CGNP-DI water nanofluid flowing in the horizontal pipe with an input heat flux of 12,752 W/m^2. The *Re* number was varied from 6371 to 15,927, indicating that the simulations were conducted for turbulent flow regime. Likewise, three CGNP weight concentrations were considered in this study, namely, 0.025, 0.075, and 0.1%. Finally, the average heat transfer coefficient was determined by inserting the average wall temperature and bulk temperature determined from simulations into Eq. (13).

Fig. 6(a) shows the comparison between numerical results and the experimental data for the average heat transfer coefficient as a function of the Reynolds number for aqueous nanofluids with various CGNP concentrations. It is seen that the average heat transfer coefficient significantly increases with an increase in the CGNP concentration. This is likely due to the thermal conductivity enhancement resulting from the Brownian motion of CGNPs suspended in DI water. Moreover, increasing the Reynolds number leads to higher average heat transfer coefficient. The greater *Re* results in higher fluid velocity and a steeper temperature gradient, which in turn, increases the heat transfer coefficient. In general, there is good agreement between the experimental and simulation data, where the average relative deviations are 8.11, 1.87, and 6.02% when the CGNP weight concentrations are 0.025, 0.075, and 0.1%, respectively.

The pressure drop across the test section was determined by inserting the wall shear stress values obtained from simulations into the Eq. (12) and the results are shown in Fig. 6(b) for various concentrations of CGNPs and *Re* numbers. It is seen that there is a slight increase in the pressure loss for the CGNPs aqueous nanofluids compared with those for DI water. In addition, the pressure drop increases slightly when the concentration of CGNPs in DI water increases. It is believed that this is caused by the slight increment in dynamic viscosity for CGNP-water nanofluids which requires a negligible increment in fluid velocity since the Reynolds number is constant. Therefore, it can be deduced that the fluid velocity plays a vital role in enhancing the pressure loss in the test section. In general, there is a good agreement between

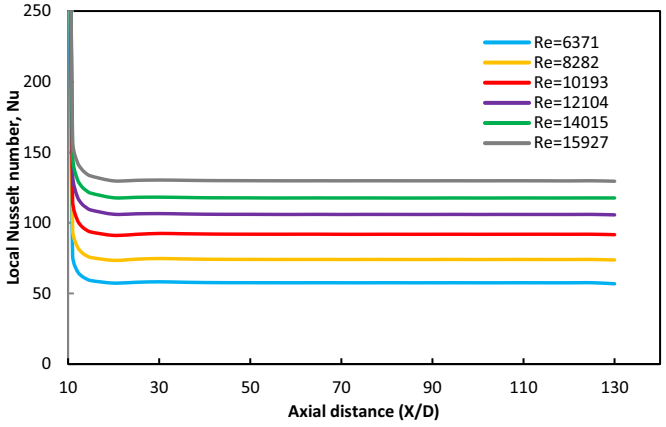

Fig. 5. Variation of the local Nusselt number along the horizontal tube for DI water in the turbulent flow regime at different *Re* numbers.

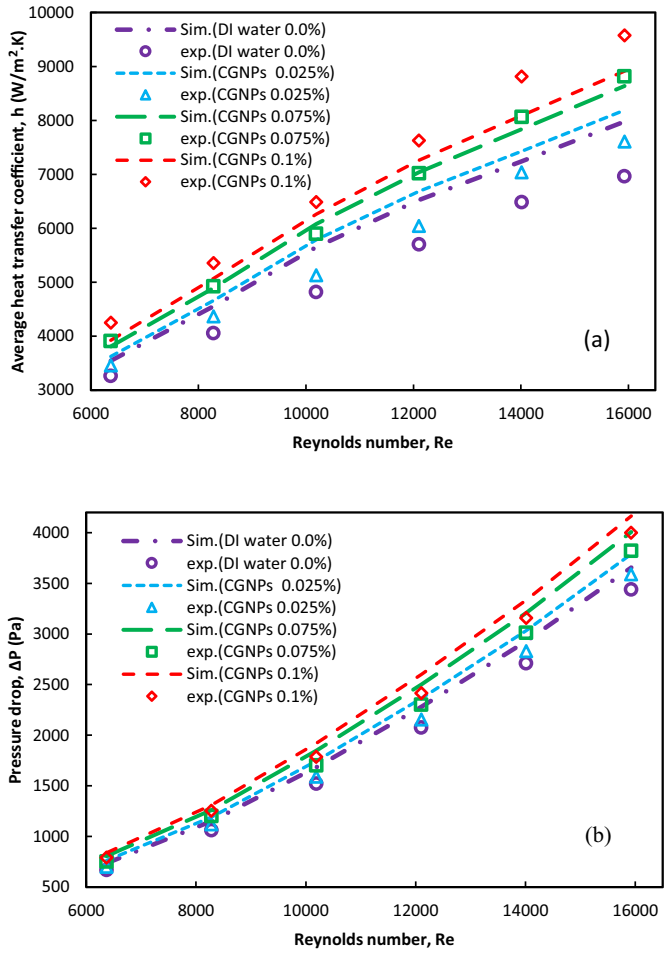

Fig. 6. Comparison of the (a) average convective heat transfer coefficient and (b) pressure drop of the CGNP-water nanofluids between simulations and experiments.

the simulation and experimental results for the pressure drops where the average relative deviations are 8.02, 6.82, and 5.94% for CGNP weight fraction of 0.025, 0.075, and 0.1%, respectively.

Fig. 7(a) and (b) shows the temperature distribution contours for the CGNP-DI water nanofluid (0.1 wt%) and DI water at $Re = 6371$, respectively, in the horizontal tube subjected to a constant heat flux of 12,752 W/m^2. The color bar showing a range of colors from blue to red indicates the temperature range from minimum to maximum in the tube. It is obvious that the inner wall temperature decreases when the CGNP/DI water nanofluids are used as the working fluids instead of DI water. In general, this reduction is due to the enhanced transport properties of the nanofluids (particularly, the higher thermal conductivity of CGNPs) and the role of Brownian motion of nanoparticles on the thermal conductivity enhancement. This in turn, leads to higher convective heat transfer enhancement, which promotes heat transfer from the higher-temperature surface (i.e. inner wall of the pipe) to the fluid. Fig. 8(a) and (b) illustrates the velocity contours for the DI water and CGNP nanofluid, respectively for the $Re = 6371$ and heat flux of 12,752 W/m^2. It is noticed that flow becomes fully developed within a short distance from the inlet due to the small diameter. In addition, the maximum velocity is higher for the CGNP nanofluid compared with that for DI water even though the Reynolds number is constant.

4. Conclusions

ANSYS Fluent commercial CFD software was used to simulate the heat transfer and friction factor of a horizontal heated tube with CGNP aqueous nanofluids as the working fluid. Here an effective single-phase turbulent flow model in conjunction with the SST k-ω model and various nanoparticle weight fractions were used in the simulations. The simulation results for the base fluid (DI water) and nanofluids were validated against experimental data as well as empirical correlations for various Reynolds numbers. Good agreement between the simulation results and the experimental data, as well as, those obtained from Notter-Rouse's and Petukhov's empirical correlations were found. The average relative deviations were 12.48, 13.72, and 11.31%, respectively, that was contributed to the existence of conduction resistance in the experimental test section, which was not considered in the CFD model, and the

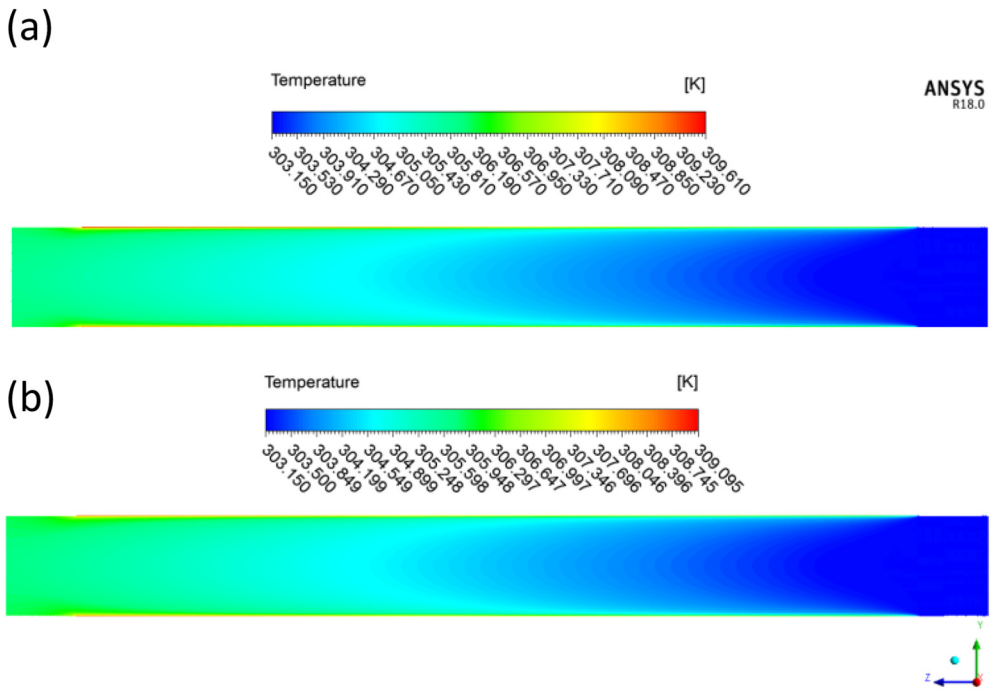

Fig. 7. Temperature distribution contours across the horizontal tube for (a) DI water and (b) CGNP nanofluid at $Re = 6371$ and uniform heat flux of 12,752 W/m^2.

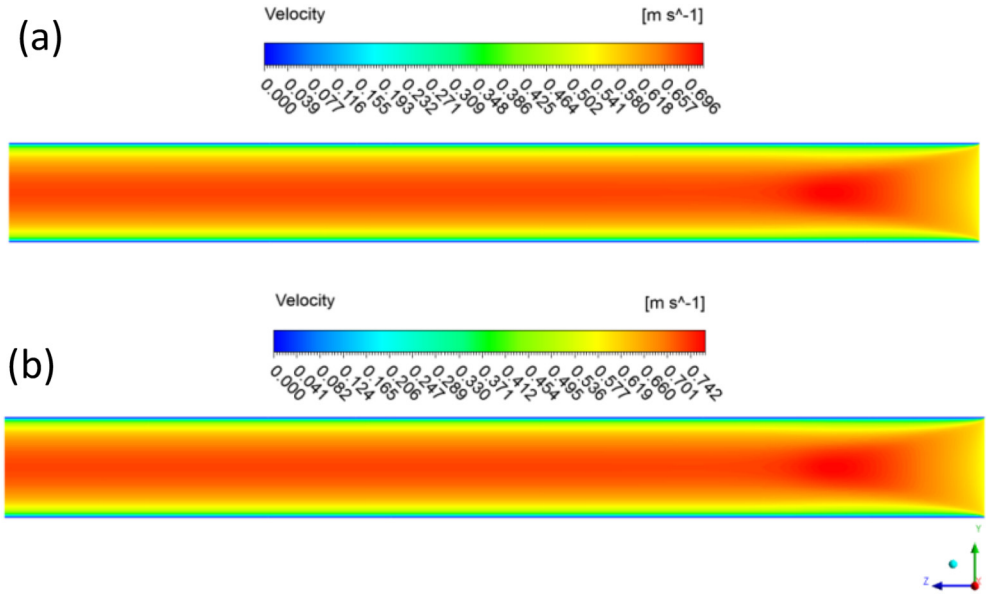

Fig. 8. Velocity distribution contours across the horizontal tube for (a) DI water and (b) CGNP nanofluid at $Re = 6371$ and uniform heat flux of 12,752 W/m^2.

turbulent model used in the simulation, besides to those resulting from the accuracy of the measurement instruments. Likewise, the average relative deviations in the friction factor between the simulations and those obtained from experiments and Petukhov's and Blasius's empirical correlations were 8.94, 6.024, and 6.56%, respectively. The results demonstrated the accuracy and reliability of the proposed CFD model for evaluating the thermal performance of the nanofluids. In general, there is good agreement between the numerical simulations and experimental results for pressure drop, with an average relative deviation of 8.02, 6.82 and 5.94% for a CGNP weight concentration of 0.025, 0.075, and 0.1%, respectively. In addition, there is a good agreement in the mean convective heat transfer coefficient with an average deviation of 8.11, 1.87 and 6.02% respectively, for a CGNP weight concentration of 0.025, 0.075, and 0.1%, respectively. Hence, we confirm that the single-phase three-dimensional CFD model developed in this study can be effectively used to predict the convective heat transfer and friction factor characteristics of CGNPs aqueous nanofluids in a horizontal heated tube.

Acknowledgment

The authors gratefully acknowledge the financial support provided by University of Malaya under Fundamental Research Grant Scheme (Project no.: FRGS-FP006-2014B) and UMRG (Project no.: RG304-14AFR).

Appendix A. Supplementary data

Supplementary data to this article can be found online at https://doi.org/10.1016/j.molliq.2018.06.011.

References

[1] M. Bahiraei, A.R. Gorjaei, A. Shahidian, Investigating heat transfer and entropy generation for mixed convection of CuO–water nanofluid in an inclined annulus, J. Mol. Liq. 248 (2017) 36–47.
[2] P. Valipour, R. Moradi, F.S. Aski, CNT-water nanofluid thermal radiation heat transfer over a stretching sheet considering heat generation, J. Mol. Liq. 237 (2017) 242–246.
[3] K. Bashirnezhad, M. Ghavami, A.A. Alrashed, Experimental investigations of nanofluids convective heat transfer in different flow regimes: a review, J. Mol. Liq. 244 (2017) 309–321.
[4] F. Khoddamrezaee, R. Motallebzadeh, D.J. Vahid, Simulation of (EG + Al_2O_3) nanofluid through the shell and tube heat exchanger with rectangular arrangement of tube and constant heat flux, J. Appl. Sci. 10 (6) (2010) 500–505.
[5] M. Amani, P. Amani, A. Kasaeian, O. Mahian, S. Wongwises, Thermal conductivity measurement of spinel-type ferrite $MnFe_2O_4$ nanofluids in the presence of a uniform magnetic field, J. Mol. Liq. 230 (2017) 121–128.
[6] S.E. Ghasemi, A. Ranjbar, M. Hosseini, Forced convective heat transfer of nanofluid as a coolant flowing through a heat sink: experimental and numerical study, J. Mol. Liq. 248 (2017) 264–270.
[7] A. Moghadassi, S.M. Hosseini, D.E. Henneke, Effect of CuO nanoparticles in enhancing the thermal conductivities of monoethylene glycol and paraffin fluids, Ind. Eng. Chem. Res. 49 (4) (2010) 1900–1904.
[8] Y. Zhang, L. Li, H. Ma, M. Yang, Effect of Brownian and thermophoretic diffusions of nanoparticles on nonequilibrium heat conduction in a nanofluid layer with periodic heat flux, Numer. Heat Transfer, Part A 56 (4) (2009) 325–341.
[9] M.H. Esfe, H. Rostamian, A novel study on rheological characteristics of non-Newtonian ZnO-MWCNT/10w40 hybrid nano-lubricant for automotive engines, J. Mol. Liq. 254 (2018) 406–413.
[10] R. Sadri, M. Hosseini, S. Kazi, S. Bagheri, N. Zubir, G. Ahmadi, M. Dahari, T. Zaharinie, A novel, eco-friendly technique for covalent functionalization of graphene nanoplatelets and the potential of their nanofluids for heat transfer applications, Chem. Phys. Lett. 675 (2017) 92–97.
[11] R. Sadri, M. Hosseini, S. Kazi, S. Bagheri, N. Zubir, K. Solangi, T. Zaharinie, A. Badarudin, A bio-based, facile approach for the preparation of covalently functionalized carbon nanotubes aqueous suspensions and their potential as heat transfer fluids, J. Colloid Interface Sci. 504 (2017) 115–123.
[12] R. Sadri, G. Ahmadi, H. Togun, M. Dahari, S.N. Kazi, E. Sadeghinezhad, N. Zubir, An experimental study on thermal conductivity and viscosity of nanofluids containing carbon nanotubes, Nanoscale Res. Lett. 9 (1) (2014) 151.
[13] M. Hosseini, R. Sadri, S.N. Kazi, S. Bagheri, N. Zubir, C. Bee Teng, T. Zaharinie, Experimental study on heat transfer and thermo-physical properties of covalently functionalized carbon nanotubes nanofluids in an annular heat exchanger: a green and novel synthesis, Energy Fuel 31 (5) (2017) 5635–5644.
[14] R. Sadri, K. Zangeneh Kamali, M. Hosseini, N. Zubir, S. Kazi, G. Ahmadi, M. Dahari, N. Huang, A. Golsheikh, Experimental study on thermo-physical and rheological properties of stable and green reduced graphene oxide nanofluids: hydrothermal assisted technique, J. Dispers. Sci. Technol. 38 (9) (2017) 1302–1310.
[15] M. Nikfar, M. Mahmoodi, Meshless local Petrov–Galerkin analysis of free convection of nanofluid in a cavity with wavy side walls, Eng. Anal. Bound. Elem. 36 (3) (2012) 433–445.
[16] A. Arefmanesh, M. Nikfar, Analysis of natural convection in a nanofluid-filled triangular enclosure induced by cold and hot sources on the walls using stabilised MLPG method, Can. J. Chem. Eng. 91 (10) (2013) 1711–1728.
[17] A. Behnampour, O.A. Akbari, M.R. Safaei, M. Ghavami, A. Marzban, G.A.S. Shabani, R. Mashayekhi, Analysis of heat transfer and nanofluid fluid flow in microchannels with trapezoidal, rectangular and triangular shaped ribs, Physica E Low Dimen. Syst. Nanostruct. 91 (2017) 15–31.
[18] V. Trisaksri, S. Wongwises, Critical review of heat transfer characteristics of nanofluids, Renew. Sust. Energ. Rev. 11 (3) (2007) 512–523.
[19] W. Daungthongsuk, S. Wongwises, A critical review of convective heat transfer of nanofluids, Renew. Sust. Energ. Rev. 11 (5) (2007) 797–817.
[20] R. Sadri, M. Hosseini, S. Kazi, S. Bagheri, S. Ahmed, G. Ahmadi, N. Zubir, M. Sayuti, M. Dahari, Study of environmentally friendly and facile functionalization of graphene nanoplatelet and its application in convective heat transfer, Energy Convers. Manag. 150 (2017) 26–36.
[21] J. Niu, C. Fu, W. Tan, Slip-flow and heat transfer of a non-Newtonian nanofluid in a microtube, PLoS One 7 (5) (2012), e37274. .

[22] M. Corcione, M. Cianfrini, A. Quintino, Heat transfer of nanofluids in turbulent pipe flow, Int. J. Therm. Sci. 56 (2012) 58–69.
[23] Q. Li, Y. Xuan, J. Wang, Investigation on convective heat transfer and flow features of nanofluids, J. Heat Transf. 125 (2003) (2003) 151–155.
[24] P.K. Namburu, D.K. Das, K.M. Tanguturi, R.S. Vajjha, Numerical study of turbulent flow and heat transfer characteristics of nanofluids considering variable properties, Int. J. Therm. Sci. 48 (2) (2009) 290–302.
[25] H. Togun, G. Ahmadi, T. Abdulrazzaq, A.J. Shkarah, S. Kazi, A. Badarudin, M. Safaei, Thermal performance of nanofluid in ducts with double forward-facing steps, J. Taiwan Inst. Chem. Eng. 47 (2015) 28–42.
[26] M.M. Rashidi, M. Nasiri, M. Khezerloo, N. Laraqi, Numerical investigation of magnetic field effect on mixed convection heat transfer of nanofluid in a channel with sinusoidal walls, J. Magn. Magn. Mater. 401 (2016) 159–168.
[27] J. Jayakumar, S. Mahajani, J. Mandal, P. Vijayan, R. Bhoi, Experimental and CFD estimation of heat transfer in helically coiled heat exchangers, Chem. Eng. Res. Des. 86 (3) (2008) 221–232.
[28] I. Conté, X. Peng, Numerical and experimental investigations of heat transfer performance of rectangular coil heat exchangers, Appl. Therm. Eng. 29 (8) (2009) 1799–1808.
[29] I. Conté, X. Peng, B. Wang, Numerical investigation of forced fluid flow and heat transfer from conically coiled pipes, Numer. Heat Transfer, Part A 53 (9) (2008) 945–965.
[30] S.E.B. Maiga, C.T. Nguyen, N. Galanis, G. Roy, Heat transfer behaviours of nanofluids in a uniformly heated tube, Superlattice. Microst. 35 (3) (2004) 543–557.
[31] R. Lotfi, Y. Saboohi, A. Rashidi, Numerical study of forced convective heat transfer of nanofluids: comparison of different approaches, Int. Commun. Heat Mass Transfer 37 (1) (2010) 74–78.
[32] A. Akbarinia, A. Behzadmehr, Numerical study of laminar mixed convection of a nanofluid in horizontal curved tubes, Appl. Therm. Eng. 27 (8–9) (2007) 1327–1337.
[33] V. Kumar, B. Faizee, M. Mridha, K. Nigam, Numerical studies of a tube-in-tube helically coiled heat exchanger, Chem. Eng. Process. Process Intensif. 47 (12) (2008) 2287–2295.
[34] I. Di Piazza, M. Ciofalo, Numerical prediction of turbulent flow and heat transfer in helically coiled pipes, Int. J. Therm. Sci. 49 (4) (2010) 653–663.
[35] M. Goodarzi, A. Amiri, M.S. Goodarzi, M.R. Safaei, A. Karimipour, E.M. Languri, M. Dahari, Investigation of heat transfer and pressure drop of a counter flow corrugated plate heat exchanger using MWCNT based nanofluids, Int. Commun. Heat Mass Transfer 66 (2015) 172–179.
[36] R. Sadri, M. Hosseini, S. Kazi, S. Bagheri, A.H. Abdelrazek, G. Ahmadi, N. Zubir, R. Ahmad, N. Abidin, A facile, bio-based, novel approach for synthesis of covalently functionalized graphene nanoplatelet nano-coolants toward improved thermo-physical and heat transfer properties, J. Colloid Interface Sci. 509 (2018) 140–152.
[37] T. Chung, Computational Fluid Dynamics, Cambridge University Press, 2010.
[38] J. Blazek, Computational Fluid Dynamics: Principles and Applications, Butterworth-Heinemann, 2015.
[39] F.R. Menter, Two-equation eddy-viscosity turbulence models for engineering applications, AIAA J. 32 (8) (1994) 1598–1605.
[40] J. Van Doormaal, G. Raithby, Enhancements of the SIMPLE method for predicting incompressible fluid flows, Numer. Heat Transfer 7 (2) (1984) 147–163.
[41] B. Petukhov, Heat transfer and friction in turbulent pipe flow with variable physical properties, Adv. Heat Tran. 6 (1970) 503–564.
[42] V. Gnielinski, New equations for heat and mass transfer in the turbulent flow in pipes and channels, NASA STI/Recon Technical Report A, 75, 1975, p. 22028.
[43] M. Khoshvaght-Aliabadi, M. Akbari, F. Hormozi, An empirical study on vortex-generator insert fitted in tubular heat exchangers with dilute Cu–water nanofluid flow, Chin. J. Chem. Eng. 24 (6) (2016) 728–736.
[44] R.H. Notter, C.A. Sleicher, A solution to the turbulent Graetz problem—III fully developed and entry region heat transfer rates, Chem. Eng. Sci. 27 (11) (1972) 2073–2093.
[45] H. Blasius, Grenzschichten in Flüssigkeiten mit kleiner Reibung, Druck von BG Teubner, 1907.